Secondary peak of downstream light field modulation caused by Gaussian mitigation pits on the rear KDP surface

HAO YANG,[1,2,4] JIAN CHENG,[1,3,4,5] ZHICHAO LIU,[2] QI LIU,[1] LINJIE ZHAO,[1] CHAO TAN,[1] JIAN WANG,[2] AND MINGJUN CHEN[1,6]

[1]*State Key Laboratory of Robotics and System, Harbin Institute of Technology, 92 West Dazhi Street, Harbin 150001, China*
[2]*Research Center of Laser Fusion, China Academy of Engineering Physics, Mianshan Road No. 64, Mianyang 621900, China*
[3]*Key Laboratory of Testing Technology for Manufacturing Process, Southwest University of Science and Technology, Mianyang 621010, China*
[4]*These authors contribute equally to this work*
[5]*cheng.826@hit.edu.cn*
[6]*chenmj@hit.edu.cn*

Abstract: Micro-milling has been proved to be the most effective method to mitigate the growth of laser-induced surface damage on potassium dihydrogen phosphate (KDP) crystals used in high power laser systems. However, the secondary peak of downstream light field modulation caused by Gaussian mitigation pits on the rear KDP surface would cause potential risk to damage downstream optics. In order to explore the effect of the mitigation pits on the secondary peak, we numerically calculated the downstream light field modulations caused by Gaussian mitigation pits on the rear KDP surface based on the angular spectrum diffraction theory. The results suggest that the secondary peaks are dependent on the parameters of the width, depth, depth error and title error. Among them, the tilt error and depth have greater influence on the mitigation effect. To reduce the laser damage risk caused by the secondary peak, the depth of the pre-designed mitigated contour should be optimized according to the actual operating conditions. The tilt error and depth error are proposed to be controlled within 1′ and 2 μm, respectively, during the micro-milling. Also, the experiments verified the calculation results of downstream modulations and the effects of these parameters on the secondary peak. This work can not only provide available models for evaluating the laser damage risk of secondary peak caused by mitigation pits on the KDP surface but also contribute to the development of optimal micro-milling parameters for laser damage mitigation as well as the installation strategy of optical components employed in the high power laser systems.

1. Introduction

Owing to the unique nonlinear optical and electro-optical properties, potassium dihydrogen phosphate (KDP for short) crystals are used in high-power laser facilities for the inertial confinement fusion (ICF) such as the National Ignition Facility in USA, Laser MegaJoule in France and Shenguang Laser Facility in China. In these laser systems, the KDP crystals are generally employed as photoelectric switches and frequency converters [1–3]. However, due to the weak mechanical and physical properties (e.g., soft and brittle, extremely water soluble, thermally sensitive, prone to fracture and scratch), it is inevitable to introduce some surface defects on KDP surfaces during the processes of machining and handling [4,5]. A large amount of these defects can contribute to the laser damage on KDP crystal when irradiated with high fluence laser [6–9]. Then, the laser damage sites would cause large optical transmittance loss, strong light-field modulation and laser beam quality reduction. As a result, high risk of laser

damage growth exists on KDP surface under subsequent multiple laser shots, especially for damage sites with macroscopic fracture [6,10,11]. The issues of laser-induced damage (LID) and damage growth for optical components have seriously affected the normal operation of ICF laser facilities [12–14]. Therefore, it is of great significance to find a suitable method for mitigating the laser-induced damage on KDP crystals to extend their service life and optical properties.

The "recycling" strategy was first proposed to maximize the lifetime of the large-aperture and high-cost optical components, which are prone to suffer from laser damage [15]. For KDP crystals, the methods, such as CO_2 laser processing, short-pulse laser ablation, aqueous wet-etching and micro-machining, were then performed to remove the initial laser damage sites for increasing their service life [15,16]. When comparing these repairing methods, the micro-machining was verified as the most promising one to repair the surface laser damage sites and mitigate their growth behavior under the subsequent laser pulse irradiations [16–18]. In order to fabricate any geometric contour to meet laser damage morphology, the micro-milling repairing technique of KDP crystal has been also developed from the initial direct dimpling to the current multi-path milling based on the numerical control code [15,17]. Although the mitigated contour could improve the laser damage resistance of the KDP crystals, Geraghty *et al*. [19] found that the repaired shallow mitigation pits on the KDP surface would alter the wave front of the outgoing light beam and cause downstream light field perturbation. Then, the effect of KDP mitigated surface on the enhancement of downstream light field was studied by Yang *et al*. [20]. The results showed that there was generally a peak of light intensity first, then a sharp decrease, and finally a stable trend, in the curves of downstream light intensification. The light intensity may rise slightly in stable region of the curve, wherein the small peak is generally defined as a secondary peak [21,22]. As for the effect of the downstream light intensifications, Guss *et al*. [23] were in belief that the light intensification greater than 3 would threaten the downstream optical elements with laser damage crisis. In order to prevent the secondary peak of downstream light intensifications, a new method for mitigating the fused silica has been developed by Bass *et al*. [24] and the downstream light intensification could be finally decreased to acceptable levels. These studies provide evidence that the secondary peak of downstream light intensification produced by the mitigated contours on fused silica is a threat to the downstream optical elements. However, the related researches on KDP crystals are relatively blank at present.

Although the secondary peak of downstream light field modulation caused by mitigated KDP crystals is much smaller than the main peak near the rear KDP surface [20,21], the secondary peak in some special cases would also pose a threat to downstream optical elements. Moreover, unlike the downstream main peak generally within 100 mm distance far from the mitigated surface, the position of the secondary peak varies greatly, which undoubtedly increases the difficulties for installing the KDP crystals after repairing. Therefore, it is significant to clarify the effect of mitigated contours on KDP surfaces on the secondary peaks of downstream light field modulations and make the corresponding standards for manufacture and application.

The mitigated contours are dependent on the pre-designed width and depth, as well as the processing errors like the depth error caused by the deviation on tool setting point and the tilt error caused by the angle between the cutter revolution plane and the KDP surface. In order to understand the relationship between mitigation pit geometry and secondary peak of downstream light field modulation, we first built a model to calculate downstream light field modulation based on the angular spectrum diffraction theory. According to the calculations corresponding to the mitigation pits with various widths, depths, depth errors and tilt errors, the effects of the secondary peaks were analyzed. The experiments were implemented by the micro-milling and downstream light field detection to verify the effect of the rear-surface Gaussian mitigation pits on the secondary peak. The results cannot only be used to comprehensively evaluate the performance of the repaired KDP crystals, but also provide technical indexes for the installation of mitigated KDP crystal and the downstream optical elements.

2. Model and theory

The repaired KDP surface with Gaussian mitigation pits would cause the disturbance in the downstream light field. In order to investigate the effect of the geometric structures of the mitigation pits on the secondary modulation peak, we utilize the scalar diffraction theory to calculate the downstream light field behind KDP surface with the mitigation pit. Figure 1 is the sketch of the far-field modulation caused by the Gaussian mitigation contour on rear KDP surface. After the beam passed through the Gaussian mitigation contour, wave turbulence would occur in the downstream light field.
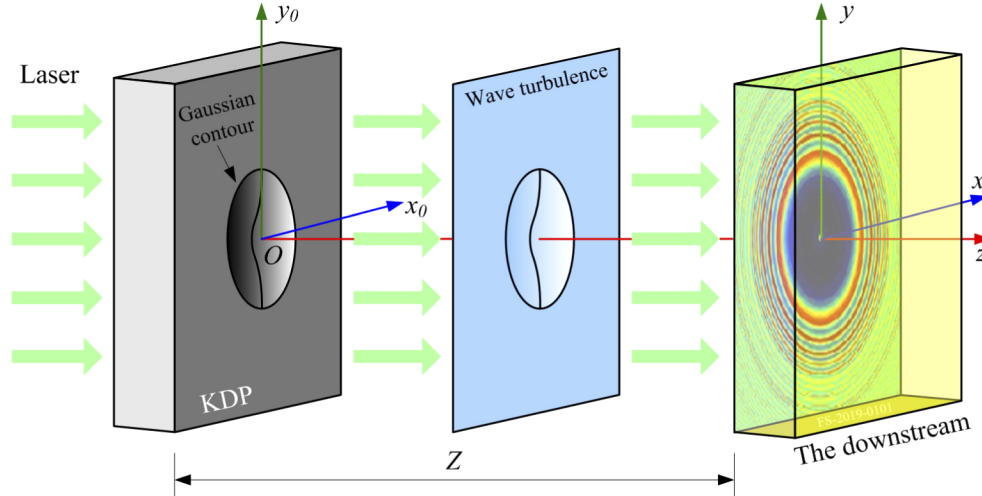

Fig. 1. Sketch of the far-field modulation caused by the Gaussian mitigation contour on rear KDP surface.

The incident laser is simplified as a uniform plane wave and propagates along the *z*-direction of the Cartesian coordinate system *o-xyz*. The diffraction distance from the rear surface of the crystal to the observation plane is Z. $U(x,y,0)$ and $U(x,y,Z)$ are the complex amplitudes of the light waves on the rear surface of the crystal and the observation plane, respectively. According to the angular spectrum diffraction theory [25,26], the transfer function in frequency domain for the beam propagating from the rear surface of the crystal to the observation plane:

$$H(f_x, f_y) = \exp\left[ikZ\sqrt{1 - (\lambda f_x)^2 - (\lambda f_y)^2} \right], \qquad (1)$$

$$f_x = \frac{x}{\lambda Z}, \quad f_y = \frac{y}{\lambda Z}, \qquad (2)$$

where λ is the wavelength of the incident laser. f_x and f_y are the coordinates of the plane wave in the *x* and *y* directions of frequency domain, respectively.

The propagation of the diffracted light field between given planes is a transformation process of linear space invariant system. Referring to the Fourier transform and inverse transform algorithm [27], the complex amplitude of the light wave on the observation plane can be expressed as:

$$U(x, y, Z) = \mathcal{F}^{-1}\{\mathcal{F}\{U(x, y, 0)\} \cdot H(f_x, f_y)\}. \qquad (3)$$

Here, $\mathcal{F}\{\dots\}$ and $\mathcal{F}^{-1}\{\dots\}$ denote the Fourier transform and the inverse Fourier transform, respectively. The (x_0, y_0) in the coordinate system of $x_0 O y_0$ in Fig. 1 is equivalent to the $(x, y, 0)$ there.

The light intensity at any point in space can be expressed as $|U|^2$ [28]. The modulation M is defined as the maximum light intensity enhancement at a distance from the rear surface of the KDP crystal. Thus, according to the initial complex amplitudes corresponding to the mitigation contour, the modulations in downstream light field are easy to calculate.

In the actual processes of KDP surface mitigation, the geometric morphology of the mitigated contour is not only related to the pre-designed parameters, but also affected by machining errors, such as the depth error Δd caused by the deviation on tool setting point (Fig. 2(a)) and the tilt error $\Delta \theta$ caused by the angle between the cutter revolution plane and the KDP surface (Fig. 2(b)). In the schematic diagrams, the dash lines and solid lines represent the pre-designed contours and the mitigated contours of the pits, respectively. The micro-milling processes generally begin at the ideal tool setting point O. During the processes, while the tilt cutter is rotating at high speed in the direction I, it also spins around in the revolution direction II. The actual tool setting point O' is always below the KDP surface, which is the main reason of depth error Δd, in Fig. 2(a). Due to the local cutting effect on the edge of the mitigation pit in the direction III of sectional view, curved steps would be generated around the mitigated counter. In Fig. 2(b), the ideal and actual revolution planes of the cutter during micro-milling are shown by the dot circles of green and black, respectively. The axis of the outline is indicated by a dash-dot line. The tilt error $\Delta \theta$ would cause a significant change to repaired morphology as the solid of mitiagated contour. The mitigation pit morphology began to become asymmetrical.
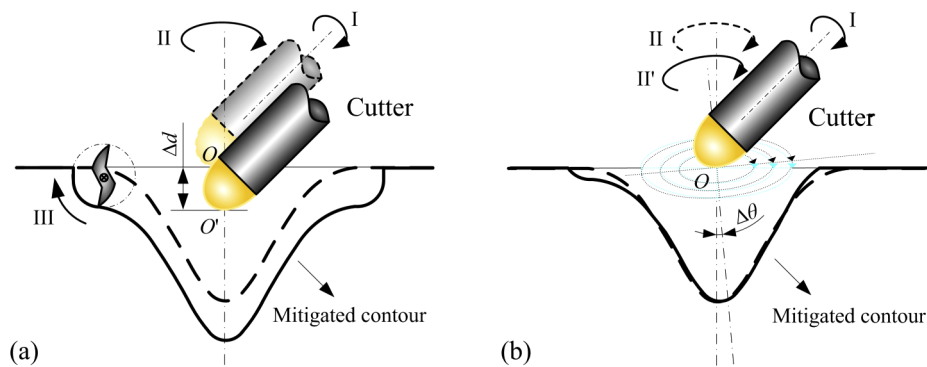

Fig. 2. Schematic diagrams of the machining error production during the mircro-milling processes on the KDP surface. (a) The depth error Δd caused by the deviation on tool setting point. (b) The tilt error $\Delta \theta$ caused by the angle between the cutter revolution plane and the KDP surface.

3. Experiment

In order to study the effect of the mitigated Gaussian contour on secondary peak of downstream light field modulation, we first fabricated the Gaussian mitigation pit on the crystal surface. Then the optical platform for detecting the distribution of downstream light field at different locations behind the mitigated surface was designed.

The Gaussian mitigation pit was fabricated on the rear KDP surface by a self-developed multi-axis micro-milling equipment [29]. The rounded Gaussian profile with the structural parameters of 800 μm width and 10 μm depth was designed. The reasons for choosing the Gaussian mitigation pit with the parameter are as follows: Firstly, there have been a few research results about the Gaussian repair contour on fused silica surface. Choosing Gaussian repair shapes helps to facilitate subsequent reference and comparison. Secondly, it is found that the width-depth ratios greater than 4.3 should be applied to the Gaussian repaired contours for optimal mitigation effects [29]. Thirdly, the maximum depth and width of the surface defects to

be repaired on the KDP crystal are less than 5 μm and 400 μm, respectively. Due to the cracks and modified material near the defect, we generally set the mitigation parameters to twice the sizes of the defect. Last but not least, the processing quality is related to the width-depth ratio of the mitigated contour. Small width-to-depth ratios would reduce the surface smoothness of the mitigation pits and even cause interference between the cutting tool and the mitigation profile. Even though there are many sets of structural parameters that meet the above criteria, the mitigation pits with large width-depth can avoid the effect of the poor surface quality on laser propagation. Adopting the structural parameters of 800 μm width and 10 μm depth, we could process high-quality repaired surfaces by using a ball-end cutter with the diameter of 500 μm. Thus, the rounded Gaussian profile with the structural parameters of 800 μm width and 10 μm depth is designed to replace the brittle fracture on the original damage site for improving the laser damage resistance of KDP surface. During the repairing process, the micro-milling cutter always maintained a high speed of 50 000 r/min, and the tool tilted an angle of 45° to the crystal surface, which ensured that the material could be milled in plastic mode and finally achieved repaired smooth surface without brittle cracks [30,31]. The depth error and tilt error were relatively random according to the system without human intervention.

Subsequently, the distributions of downstream light field at different locations behind the mitigated KDP surface were detected with the light path in Fig. 3. The laser outputted a continuous laser beam with a wavelength of 527nm. Then, the laser was spatially filtered and collimated by using the aperture and lens. The laser spot diameter that applied to irradiate the mitigated KDP crystal was ~ 5 mm. The Gaussian mitigation pit on the KDP surface was able to be completely covered by the laser spot. After the laser passing through the mitigated KDP sample, the diffraction patterns induced by the laser light perturbation would be imaged onto a digital CCD camera.
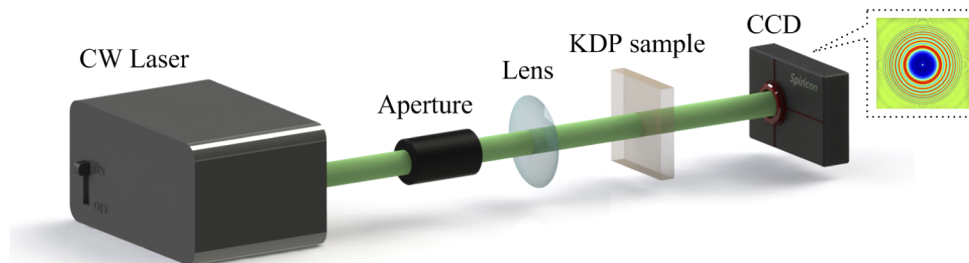

Fig. 3. Light path for detecting the distribution of downstream light field at different locations.

4. Results and discussion

4.1. Effect of the repair width on the secondary peak

The scalar diffraction theory was used to calculate the downstream light field modulation behind rear KDP surface with the Gaussian mitigation pits. Figure 4 shows the curves of downstream light field modulation with respect to laser propagation distance caused by the Gaussian mitigation pits with the depth of 10 μm and width of 800 μm, 1000 μm and 1200 μm, respectively. The three curves are almost parallel. As the propagation distance from the rear surface increases, the light field modulation increases sharply first, and then decreases to a stable value. When the curve of downstream light field modulation tends to be stable, the secondary peak appears. The inset is a partial enlargement of the modulation curves near the secondary peak. When the width of the repaired contour increases, the secondary peak of the modulation curve increases slightly. As for the mitigation pits with the width of 800 μm and 1200 μm, they are ~2.2 and

~2.8, respectively. The modulation increases by 27%, which is not so big compared to the 50% increment in width. The diffraction pattern shown in the inset of Fig. 4 describes the light intensity distribution caused by the mitigation pit with the width of 1200 μm and depth of 10 μm at the position where the downstream secondary peak modulation is. Light intensifications are caused by on-axis hot spot and off-axis ring caustic in the diffracted field [24,32], which are clear in this pattern. The maximum light intensity is at the center of the diffraction pattern. This indicates that the repair width increment results in the enhancement of the on-axis hot spot at the far position of the diffraction. Previous studies have also suggested that the on-axis hot spot is related to the overall contour of the repaired area [32]. Thus, it can be believed that the secondary peak due to the width increase is related to the on-axis hot spot that generated by diffraction. Besides, the modulations of the secondary peaks are too small to cause laser damage. It could not be paid more attention in the optics installation.
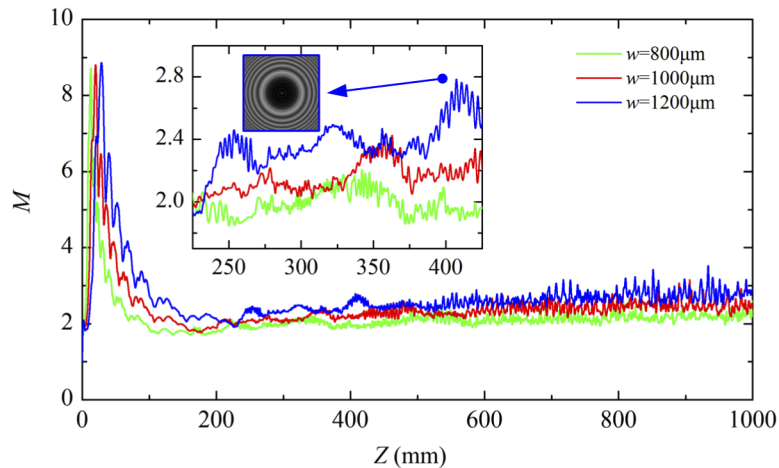

Fig. 4. Modulation curves of downstream light field modulation with respect to propagation distance caused by the Gaussian mitigation pits with depth of 10 μm and widths of 800 μm, 1000 μm and 1200 μm, respectively. The inset is a partial enlargement of the modulation curves near the secondary peak, wherein the inserted diffraction pattern describes the light intensity distribution caused by the mitigation pit with the width of 1200 μm and depth of 10 μm at the position corresponding to the secondary peak.

4.2. Effect of the repair depth on the secondary peak

In order to determine the effect of the repair depth on the secondary peak, we calculated the downstream light field modulation caused by the Gaussian mitigation pits with the width of 800 μm and depths of 10 μm, 20 μm and 30 μm, respectively. Figure 5 is the curves of downstream light field modulation with respect to laser propagation distance. Different from the effect of the width variation of Gaussian mitigation pit on the rear KDP surface on the downstream light field modulation, the modulation degree is more sensitive to the depth variation of the Gaussian mitigation pit. The inset is a partial enlargement of the modulation curves near the secondary peak. The secondary peaks of the downstream light field modulation generated by the Gaussian mitigation pits with widths of 10 μm, 20 μm and 30 μm are ~2.2, ~4 and ~2.6, respectively. The modulation degree of light field increases firstly and then decreases with the increase of the repairing depth. Its growth is nonlinear. From the secondary peak values of the light field modulation, they increase significantly as the depths of mitigation pits increase. The repair depth doubles from 10 μm to 20 μm. Then, the secondary peak gets 82% higher. Thus, the depth variation has more influence on the secondary peak than the width variation. The cross section of

light intensity distribution at the position corresponding to the secondary peak of the modulation curve for the Gaussian mitigation pit with the width of 800 μm and depth of 20 μm is shown in the inserted diffraction pattern in Fig. 5. As can be clearly seen from the pattern, the on-axis hot spot dominates with the largest light intensity. The light intensity contrast is even more obvious than that in the diffraction pattern of Fig. 4. The increase of the repair depth introduces more phase components, which contributed to the enhancement of diffraction. However, for some special damage points, deep mitigation contours should be designed for damage material removal. Thus, for deeper Gaussian mitigation pits, it is important to reasonably avoid the secondary peak of the downstream light intensification.
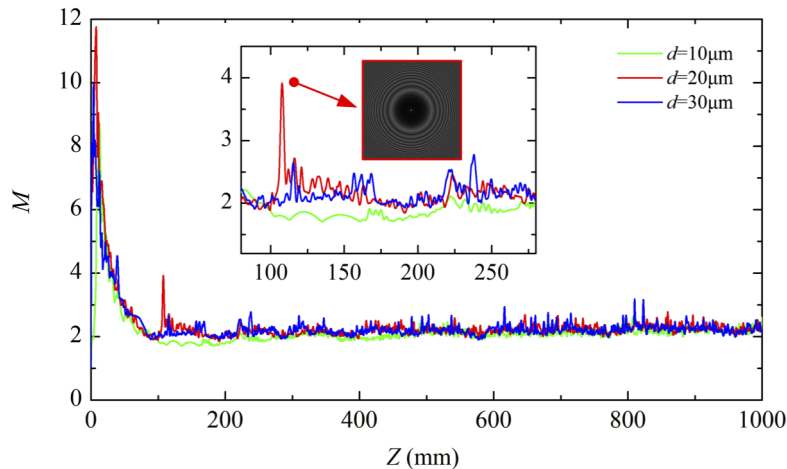

Fig. 5. Modulation curves of downstream light field with respect to laser propagation distance caused by the Gaussian mitigation pits with the width of 800 μm and depths of 10 μm, 20 μm and 30 μm, respectively. The inset is a partial enlargement of the modulation curves near the secondary peak, wherein the inserted diffraction pattern describes the light intensity distribution caused by the mitigation pit with width of 800 μm and depth of 20 μm at the position corresponding to the secondary peak.

4.3.   *Effect of the depth error on the secondary peak*

The solving results of the downstream light field modulation can be seen in Fig. 6. The three curves correspond to the Gaussian mitigation pits with the depth error Δd of 0, 1 μm and 2 μm, respectively. All these curves rise slightly after 100mm. From the inset, the modulation of $\Delta d = 1$ μm increases the most among the range from 100 mm to 300mm. Compared with the secondary peak of $\Delta d = 0$, its value adds from 2.2 to 2.4. But as Δd increases to 2 μm, the secondary peak is not larger than that of $\Delta d = 1$ μm, even with some slight decline. This is similar to the effect of depth on the variation of the secondary peak. The depth error would alter the overall depth of the mitigation pit, which should be the reason for the similarity. However, different from the repair depth variation, the depth error only changes the local details of the contour. Thus, the depth error plays a minor effect on the secondary peak. As for the depth error less than 2, their secondary peaks are all less than 3. The modulations are safe for downstream optical elements. The inserted diffraction pattern describes the light intensity distribution caused by the mitigation pit with $\Delta d = 1$ μm at the position corresponding to the secondary peak. The maximum light intensity is located on the off-axis ring caustic. The off-axis ring caustic is mainly due to the arc contour around the mitigation pit, which produces the effects like a convex lens [32,33]. According to the theoretical analysis (Fig. 2(a)) in the Section 2, the depth error would generate curved steps at the

edge of the repaired contour. This is the reason why the secondary peak rise with the depth error added. Due to the lower enhancement of the secondary peak, depth errors less than 2 µm caused by the deviation on tool setting point are acceptable in the actual micro-milling process.
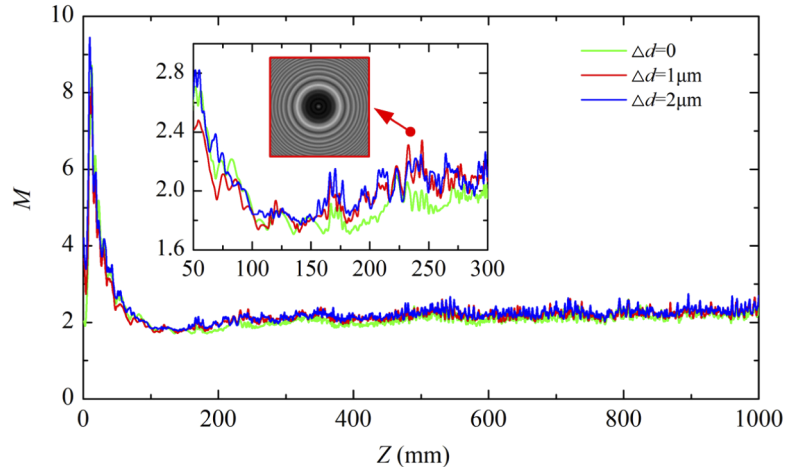

Fig. 6. Modulation curves of downstream light field with respect to laser propagation distance caused by the Gaussian mitigation pits with the depth error Δd of 0, 1 µm and 2 µm, respectively. The inset is a partial enlargement of the modulation curves near the secondary peak, wherein the inserted diffraction pattern describes the light intensity distribution caused by the mitigation pit with $\Delta d = 1$ µm at the position corresponding to the secondary peak.

4.4.   Effect of the tilt error on the secondary peak

The modulation curves of downstream light field with respect to laser propagation distance are exhibited in Fig. 7. These three curves correspond to the Gaussian mitigation pits with the tilt error $\Delta\theta$ of 0, 1′ and 2′, respectively. In general, as the tilt error of the mitigation pit increases, the tendencies of other modulation curves are nearly the same with the modulation over that of $\Delta\theta = 0$. And these two curves fluctuate strongly. When $\Delta\theta = 1′$, the curve increases the most and the secondary peak is greater than 3. The curve of $\Delta\theta = 2′$ almost overlaps with the curve of $\Delta\theta = 1′$, with the secondary peak a little bit smaller. The results suggest that the small variation of tilt error would have great influence on the modulation. It is because that the tilt error results in a great change in the geometry of the mitigated contour. As shown in Fig. 2(b), the contour of perfect spatial symmetry is broken. When a light beam passes through the surface, it is easier to generate diffraction points with high light intensity. The inserted diffraction pattern is the light intensity distribution caused by the mitigation pit with $\Delta\theta = 1′$ at the position corresponding to the secondary peak. Due to the tilt of the repaired profile, the bright rings are slightly offset to one side, and not perfect concentric. The on-axis hot spot is also off the center with the largest light intensity. The modulation degree exceeds 3, which would cause ionization breakdown or high-temperature ablation for the downstream optics, resulting in irreversible material damage. Thus, the tilt error should be controlled within 1′.

4.5.   Experiment on the downstream light field modulation

The Gaussian mitigation pit on the KDP surface was first fabricated. Considering the influence of machined surface quality on downstream light field modulation, we selected a mitigation pit with larger width-depth ratio under the premise of meeting the basic criteria of width-depth
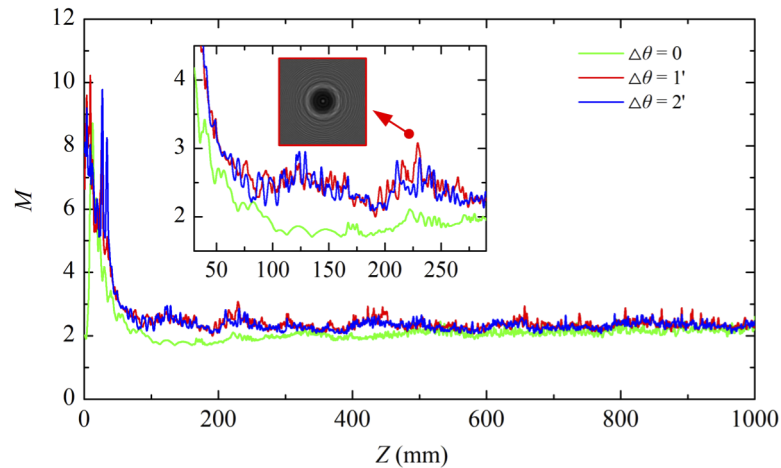
Fig. 7. Modulation curves of downstream light field with respect to laser propagation distance caused by the Gaussian mitigation pits with the tilt error $\Delta\theta$ of 0, 1′ and 2′, respectively. The inset is a partial enlargement of the modulation curves near the secondary peak, wherein the inserted diffraction pattern describes the light intensity distribution caused by the mitigation pit with depth error $\Delta\theta = 1′$ at the position corresponding to the secondary peak.

ratio. Figure 8 is microscopic morphology of the manufactured surface observed by the micro-profilometer. The three-dimensional contour of the whole mitigation pit is displayed in Fig. 8(a). In general, the mitigation pit is of good machining quality, with smooth surface and no burrs. Its surface roughness is controlled under 30 nm. The geometric contour after micro-milling processes in the three-dimensional view can show the characteristics of the pre-designed Gaussian contour. Due to the depth error and tilt error in the machining process, the overall mitigated contour is inclined with the curved steps on the edges, which can be seen in Fig. 8(b). The depth error Δd and tilt error $\Delta\theta$ are 8.13 μm and 4.42′, respectively. Besides, both the width and the depth of the Gaussian mitigation pits expand for that reason.
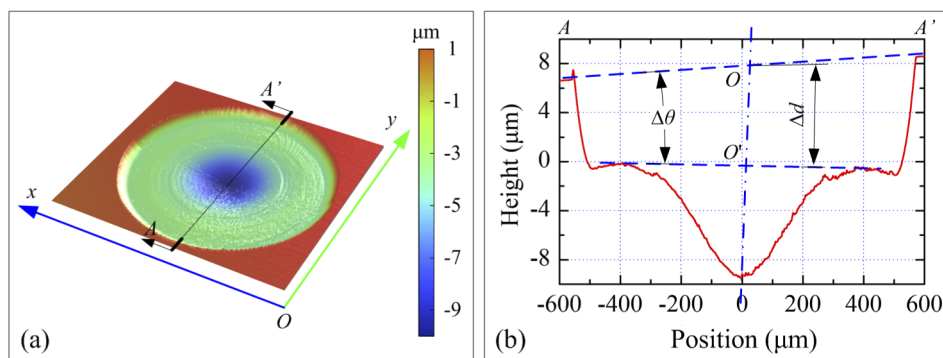

Fig. 8. Microscopic morphology of the manufactured Gaussian mitigation pit. (a) The three-dimensional contour. (b) The two-dimensional profile.

Using the testing morphology of the fabricated Gaussian mitigation pit in Fig. 8, we have simulated the downstream light field modulation caused by the mitigated contour. Since the same mitigation pit is used in the experiments of downstream light intensity detection, it is believed

that the structure parameters of the mitigation contours used for experiment and simulation are consistent. The calculations and experiments on the downstream light field modulation are shown in Fig. 9. In the graph, they are represented by the blue curve and the red curve, respectively. As we can see, these two curves show similar trends. With the light propagation distance 10 mm < Z < 50 mm, the curves drop steeply. When Z is more than 50 mm, there are three peaks (I, II and III in the graph) in both of them. Besides, the three peaks increase with the diffraction distance. The maximum of them is located in a position ~180 mm far from the rear KDP surface. The modulations of the calculations and the experiments in this distance are greater than 5. It would threaten the downstream optics with laser damage crisis in the engineering application. With Z over 400 mm, the curves tend to be stable. The experimental results in the blue, green and red regions correspond to the diffraction patterns on the right, respectively. The light propagation distance Z of the diffraction patterns in the first blue row is 50 mm ~ 70 mm (Figs. 9(a)-(c)). The brightness of the off-axis ring caustic in these patterns gradually increases. According to the analysis in Section 4.3, the arc edge due to the depth error is a major cause. Although the depth error is 8.13 μm, the induced modulation does not increase much. Thus, it suggests that the depth error has limited influence on the secondary peak, and the standard of depth error less than 2 μm is safe enough. The diffraction patterns in the second green row are corresponding to Z of 70 mm ~ 100 mm (Figs. 9(d)-(f)), with the modulation larger than the first blue row. There is an on-axis hot spot in the center of the pattern with the highlight. As for diffraction patterns in the third red row corresponding to Z of 100 mm ~ 200 mm (Figs. 9(g)-(i)), the maximum light intensity is still in the center. The difference is that the modulation has increased significantly. The offset on-axis hot spot can be used as evidence that the tilt error would increase the secondary peak. But both the width and depth also contribute to on-axis hot spot in the far-field. Thus, the modulation in the peak II and the peak III can be considered as a combination effect of all three. The maximum modulation in the peak III is very big, which demonstrates the effects of width, depth, and tilt error. According to the simulation results, the tilt error should be controlled below 1′. The width and depth can be designed based on the actual damage site and the secondary peak should be avoided in the application.
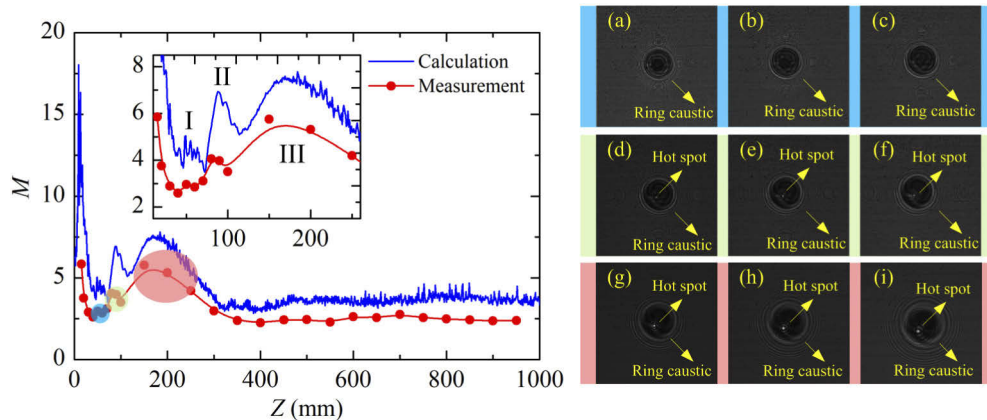

Fig. 9. Comparison between the calculations and experiments. The curves of downstream light field modulation caused by the manufactured Gaussian mitigation pit on the rear KDP surface are displayed in the graph. The blue represents the calculation results of downstream light field modulation. The red one is fitted according to the experimental data. The diffraction patterns (a-i) on the right side are obtained by experimental detection. The photographs in each row are correspond to locations inside the regions with the same color in the left graph.

As for the error between experiments and simulations, it may be due to the influence of stray light during the experiment. In a word, the experiments verify the correctness of the simulations to some extent. What's more, the research proves that the morphology factor of the Gaussian mitigation pits, such as the depth, the width, the depth error and the tilt error would affect the secondary peak of the downstream light field modulation.

5. Conclusion

The effects of Gaussian mitigation pits on the rear surface of KDP crystals with various width, depth, depth error and tilt error on the secondary peak of downstream light field modulation were theoretically and experimentally investigated. The depth error would strengthen the off-axis ring caustic and increase the secondary peak. The other parameters of the width, depth and tilt error affect the secondary peak mainly due to the modulation at the on-axis hot spot. The modulation variation of the secondary peak caused by the width and depth error is small. The depth error less than 2 μm can be acceptable. When the components actually installing, it is unnecessary to worry about the width variation on the secondary peak, and the modulation would not affect the downstream optical components generally. However, the depth and the tilt error play vital roles in the secondary peak. In order to ensure the safety of system operation, the tilt error of the mitigated contour is supposed to be controlled within 1′. The depth should also be optimized according to the operating conditions. The experimental results also well verified the simulations based on the diffraction theory, as well as the structure parameter effects of the Gaussian mitigation pit on the secondary peak. This work provides further insights in understanding the mitigation effects of the Gaussian contours on the KDP surface by micro-milling. Besides, the conclusions could also be referenced in the engineering applications like mitigation pits fabrication or optics element installation.

Disclosures

The authors declare no conflicts of interest.

References

1. R. A. Hawley-Fedder, P. Geraghty, S. N. Locke, M. S. McBurney, M. J. Runkel, T. I. Suratwala, S. L. Thompson, P. J. Wegner, and P. K. Whitman, "NIF Pockels cell and frequency conversion crystals," Proc. SPIE **5341**, 121–126 (2004).
2. E. I. Moses, "Advances in inertial confinement fusion at the National Ignition Facility (NIF)," Fusion Eng. Des. **85**(7-9), 983–986 (2010).
3. D. Besnard, "The megajoule laser program — ignition at hand," Eur. Phys. J. D **44**(2), 207–213 (2007).
4. J. J. De Yoreo, A. K. Burnham, and P. K. Whitman, "Developing KH_2PO_4 and KD_2PO_4 crystals for the world's most powerful laser," Int. Mater. Rev. **47**(3), 113–152 (2002).
5. Z. Zhu, S. To, W. Zhu, P. Huang, and X. Zhou, "Cutting forces in fast-/slow tool servo diamond turning of micro-structured surfaces," Int. J. Mach. Tool. Manu. **136**, 62–75 (2019).
6. K. R. Manes, M. L. Spaeth, J. J. Adams, M. W. Bowers, J. D. Bude, C. W. Carr, A. D. Conder, D. A. Cross, S. G. Demos, J. M. G. D. Nicola, S. N. Dixit, E. Feigenbaum, R. G. Finucane, G. M. Guss, M. A. Henesian, J. Honig, D. H. Kalantar, L. M. Kegelmeyer, Z. M. Liao, B. J. MacGowan, M. J. Matthews, K. P. McCandless, N. C. Mehta, P. E. Miller, R. A. Negres, M. A. Norton, M. C. Nostrand, C. D. Orth, R. A. Sacks, M. J. Shaw, L. R. Siegel, C. J. Stolz, T. I. Suratwala, J. B. Trenholme, P. J. Wegner, P. K. Whitman, C. C. Widmayer, and S. T. Yang, "Damage mechanisms avoided or managed for NIF large optics," Fusion Sci. Technol. **69**(1), 146–249 (2016).

7. J. Cheng, M. Chen, W. Liao, H. Wang, J. Wang, Y. Xiao, and M. Li, "Influence of surface cracks on laser-induced damage resistance of brittle KH_2PO_4 crystal," Opt. Express **22**(23), 28740–28755 (2014).

8. H. Yang, J. cheng, Z. Liu, Q. Liu, L. Zhao, J. Wang, and M. chen, "Dynamic behavior modeling of laser-induced damage initiated by surface defects on KDP crystals under nanosecond laser irradiation," Sci. Rep. **10**(1), 500 (2020).

9. J. Bude, C. W. Carr, P. E. Miller, T. Parham, P. Whitman, M. Monticelli, R. Raman, D. Cross, B. Welday, F. Ravizza, T. Suratwala, J. Davis, M. Fischer, R. Hawley, H. Lee, M. Matthews, M. Norton, M. Nostrand, D. Vanblarcom, and S. Sommer, "Particle damage sources for fused silica optics and their mitigation on high energy laser systems," Opt. Express **25**(10), 11414–11435 (2017).

10. S. G. Demos, M. R. Kozlowski, M. Staggs, L. L. Chase, A. Bumham, and H. B. Radousky, "Mechanisms to explain damage growth in optical materials," Proc. SPIE **4347**, 277–284 (2001).

11. K. Wang, B. Ma, J. Han, H. Jiao, X. Cheng, and Z. Wang, "Morphological and damage growth characteristics of shell-type damage of fused silica optics induced by ultraviolet laser pulses," Appl. Opt. **58**(32), 8882–8888 (2019).

12. H. Bercegol, A. Boscheron, J. Di-Nicola, E. Journot, L. Lamaignère, J. Néauport, and G. Razé, "Laser damage phenomena relevant to the design and operation of an ICF laser driver," J. Phys.: Conf. Ser. **112**(3), 032013 (2008).

13. L. Lamaignère, M. Chambonneau, R. Diaz, R. Courchinoux, and T. Donval, "Laser damage resistance qualification of large optics for high power laser," Proc. SPIE **9345**, 934508 (2015).

14. J. Yu, X. Xiang, S. He, X. Yuan, W. Zheng, H. Lv, and X. Zu, "Laser-induced damage initiation and growth of optical materials," Adv. Cond. Matter. Phys. **2014**, 1–10 (2014).

15. M. L. Spaeth, P. J. Wegner, T. I. Suratwala, M. C. Nostrand, J. D. Bude, A. D. Conder, J. A. Folta, J. E. Heebner, L. M. Kegelmeyer, B. J. MacGowan, D. C. Mason, M. J. Matthews, and P. K. Whitman, "Optics recycle loop strategy for NIF operations above UV laser-induced damage threshold," Fusion Sci. Technol. **69**(1), 265–294 (2016).

16. L. W. Hrubesh, R. B. Brusasco, W. Grundler, M. A. Norton, E. E. Donohue, W. A. Molander, S. L. Thompson, S. R. Strodtbeck, P. K. Whitman, M. D. Shirk, P. J. Wegner, M. C. Nostrand, and A. K. Burnham, "Methods for mitigating growth of laser-initiated surface damage on DKDP optics at 351 nm," Proc. SPIE **4923**, 180–191 (2002).

17. J. Cheng, M. Chen, W. Liao, H. Wang, Y. Xiao, and M. Li, "Fabrication of spherical mitigation pit on KH_2PO_4 crystal by micro-milling and modeling of its induced light intensification," Opt. Express **21**(14), 16799–16813 (2013).

18. S. Elhadj, W. A. Steele, D. S. Vanblarcom, R. A. Hawley, K. I. Schaffers, and P. Geraghty, "Scalable process for mitigation of laser-damaged potassium dihydrogen phosphate crystal optic surfaces with removal of damaged antireflective coating," Appl. Opt. **56**(8), 2217–2225 (2017).

19. P. Geraghty, W. Carr, V. Draggoo, R. Hackel, C. Mailhiot, and M. Norton, "Surface damage growth mitigation on KDP/DKDP optics using single-crystal diamond micro-machining ball end mill contouring," Proc. SPIE **6403**, 64030Q (2006).

20. H. Yang, J. Cheng, M. Chen, Q. Liu, Z. Liu, J. Wang, and Q. Xu, "Downstream light intensification induced by Gaussian mitigation pits using micro-milling on rear KDP surface," Proc. SPIE **10840**, 61 (2019).

21. Y. Bai, L. Zhang, W. Liao, H. Zhou, C. Zhang, J. Chen, Y. Ye, Y. Jiang, H. Wang, X. Luan, X. Yuan, and W. Zheng, "Study of downstream light intensity modulation by mitigated damage pits of fused silica using numerical simulation and experimental measurements," Acta. Phys. Sin. **65**, 24205 (2016).

22. Y. Zheng, P. Ma, H. Li, Z. Liu, and S. Chen, "Studies on transmitted beam modulation effect from laser induced damage on fused silica optics," Opt. Express **21**(14), 16605–14 (2013).

23. G. Guss, I. Bass, V. Draggoo, R. Hackel, S. Payne, M. Lancaster, and P. Mak, "Mitigation of growth of laser initiated surface damage in fused silica using a 4.6µm wavelength laser," Proc. SPIE **6403**, 64030M (2006).

24. I. L. Bass, G. M. Guss, M. J. Nostrand, and P. J. Wegner, "An improved method of mitigating laser induced surface damage growth in fused silica using a rastered pulsed CO_2 laser," Proc. SPIE **7842**, 784220 (2010).

25. J. Li, *Diffraction calculation and digital holography* (Science Press, 2014).

26. F. Tournemenne, S. Bouillet, C. Rouyer, C. Leymarie, J. Iriondo, B. Da Costa Fernandes, G. Gaborit, B. Battelier, and N. Bonod, "Strong light intensifications yielded by arbitrary defects: Fresnel diffraction theory applied to a set of opaque disks," Phys. Rev. Appl. **11**(3), 034008 (2019).

27. J. Li, C. Yuan, P. Tankam, and P. Picart, "The calculation research of classical diffraction formulas in convolution form," Opt. Commun. **284**(13), 3202–3206 (2011).

28. M. Born and E. Wolf, Principles of optics: electromagnetic theory of propagation, interference and diffraction of light (Elsevier, 2013).

29. H. Yang, J. Cheng, M. Chen, J. Wang, Z. Liu, C. An, Y. Zheng, K. Hu, and Q. Liu, "Optimization of morphological parameters for mitigation pits on rear KDP surface: experiments and numerical modeling," Opt. Express **25**(15), 18332–18345 (2017).

30. Y. Xiao, M. Chen, Y. Yang, and J. Cheng, "Research on the critical condition of Brittle-Ductile Transition about Micro-Milling of KDP crystal and experimental verification," Int. J. Precis. Eng. Man. **16**(2), 351–359 (2015).

31. Q. Liu, J. Cheng, Y. Xiao, M. Chen, H. Yang, and J. Wang, "Effect of tool inclination on surface quality of KDP crystal processed by micro ball-end milling," Int. J. Adv. Manuf. Tech. online (2018).

32. M. J. Matthews, I. L. Bass, G. M. Guss, C. C. Widmayer, and F. L. Ravizza, "Downstream intensification effects associated with CO2 laser mitigation of fused silica," Proc. SPIE **6720**, 67200A (2007).

33. Y. Jiang, Q. Zhou, R. Qi, X. Gao, H. Wang, C. Yao, J. Wang, X. Zhao, C. Liu, X. Xiang, X. Zu, X. Yuan, and X. Miao, "Influence of secondary treatment with CO_2 laser irradiation for mitigation site on fused silica surface," Chin. Phys. B **25**(10), 108104 (2016).